Which of Three Voltammetric Methods, When Applied to a Reversible Electrode Reaction, Can Best Cope with Double-Layer Capacitance and Severe Uncompensated Resistance?

ARTICLE *in* ANALYTICAL CHEMISTRY · AUGUST 2000

Impact Factor: 5.64 · DOI: 10.1021/ac991400b · Source: PubMed

2 AUTHORS:

Jan C. Myland
Trent University
107 PUBLICATIONS **1,202** CITATIONS
SEE PROFILE

Keith Oldham
Trent University
271 PUBLICATIONS **8,462** CITATIONS
SEE PROFILE

Anal. Chem. **2000,** *72,* 3210−3217

Which of Three Voltammetric Methods, When Applied to a Reversible Electrode Reaction, Can Best Cope with Double-Layer Capacitance and Severe Uncompensated Resistance?

Jan C. Myland and Keith B. Oldham*

Department of Chemistry, Trent University, Peterborough, ON, Canada K9J 7B8

The presence of uncompensated resistance and double-layer capacitance confounds the accurate measurements of the bulk concentration of electroreactant and the reversible half-wave potential from an experimental voltammogram. It is pertinent to ask which simple voltammetric technique—chronopotentiometry, linear-scan voltammetry, or potential-step voltammetry—is best able to confront these difficulties. We have carried out a modeling study in an attempt to answer this question. First, we devised an exact method of simulating each variety of reversible voltammogram, incorporating the effects of resistance and capacitance. Next, we developed an unprejudiced method of analyzing these voltammograms to recover both electrochemical parameters. Then we performed a sensitivity analysis on a very large number of simulated voltammograms by measuring the apparent half-wave potential and concentration when slightly erroneous values of resistance and capacitance were employed in the recovery step. Thereby we hoped to ascertain how uncertainty in the magnitudes of the two interfering electrical elements affects the measured values of the two electrochemical parameters. Basing conclusions on the sizes of the four sensitivity indices, we conclude, surprisingly, that linear-scan voltammetry, not chronopotentiometry, is most often the method of choice.

Voltammetry is an important tool in electroanalysis and in the measurement of electrochemical parameters. However, the inevitable presence of electrode capacitance and uncompensated resistance undermines the precision with which measurements may be made. Of course, careful construction and placement of the reference electrode can minimize uncompensated resistance and instrumental alleviation of the problem via positive feedback[1,2] is another useful tactic. Nevertheless, there are circumstances, especially when electrochemistry is carried out in media of low conductivity or when the electrode material is itself inherently resistive, in which uncompensated resistances in the tens of kilohms must be confronted. One approach is to measure,[3] or estimate,[4] the uncompensated resistance and incorporate this resistance value into a model with which the experimental voltammogram is then compared. For the most part, such models have used digital simulation.[5] Here we adopt a similar philosophy, but use convolutive modeling[6,7] in addressing the question that forms the title of this article.

To delimit the investigation, we will assume that the electrode reaction is an uncomplicated, reversible, *n*-electron transfer

$$\mathrm{R(soln)} - n\mathrm{e}^- \rightarrow \mathrm{P(soln)} \qquad (1)$$

Furthermore, it will be assumed that the electrode is effectively planar and that transport is solely by planar semiinfinite diffusion. If the reversibility of reaction 1 is not in doubt, there can only be one of two objectives of the voltammetric investigation: either to determine one member of the composite constant $nFAc_R^b(D_R)^{1/2}$ or to measure the half-wave potential $E_{1/2}$. Here F and A denote Faraday's constant and the electrode area. We symbolize the bulk concentration and diffusivity of species i by c_i^b and D_i. More often than not, it is the c_R^b term that is the sought component of the composite constant and henceforth we assume this to be the case.

So that the initial conditions of the experiment are well characterized, we will assume that, as well as the reactant, the product P is present initially, though at a concentration c_P^b that is not analytically significant. It is, however, sufficient to establish a stable, known, null potential E_n at which the system rests prior to the voltammetry. To provide realism, we suppose that only a limited potential window, of width $2n(E_{1/2} - E_n)$ and centered at $E_{1/2}$, is available to the experimenter. In all our examples, this width is fixed at $(600/n)$ millivolts.

The goal is to measure either the bulk reactant concentration or the half-wave potential. Information on the former is richest in the "plateau" region of a voltammogram where concentration polarization is intense. On the other hand, no information relevant to $E_{1/2}$ is available from measurements on the plateau; instead, it is to the "escarpment" region of the voltammogram, where thermodynamics and transport are comparably important, that we must look for such information. Accordingly, voltammetric methods that "sweep" the electrode potential across the accessible

(1) He, P.; Faulkner, L. R. *Anal. Chem.* **1986**, *59*, 717.
(2) Roe. D. K. In *Laboratory techniques in electroanalytical chemistry*; Kissinger, P. T., Heineman, W. R., Eds.; Dekker: New York, 1996.
(3) McDonald, J. R. *Impedance Spectroscopy*; Wiley: New York, 1987.
(4) Bond, A. M.; Oldham, K. B.; Snook, G. *Anal. Chem.*, submitted.
(5) Bond, A. M.; Feldberg, S. W. *J. Phys. Chem. B* **1998**, *102*, 9966.
(6) Mahon, P. J.; Oldham, K. B. *J. Electroanal. Chem.* **1998**, *445*, 179.
(7) Mahon, P. J.; Oldham, K. B. *J. Electroanal. Chem.* **1999**, *464*, 1.

10.1021/ac991400b CCC: $19.00
Published on Web 06/08/2000

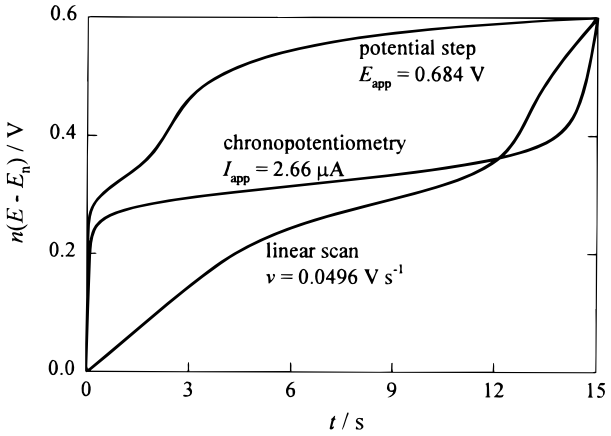

Figure 1. A graph showing typical variations with time of the electrode potential, E, during the three rival techniques. Note that these are *not* voltammograms, because the electrode potential is *not* an observable quantity in the presence of uncompensated resistance. Parameters used in drawing these curves: $n = 1$, $A = 3.698 \times 10^{-6}$ m^2, $T = 298.15$ K, $D_R = 1.000 \times 10^{-9}$ m^2 s^{-1}, $E_n = 0.000$ V, $E_{1/2} = 0.300$ V, $c_R^b = 1.000$ mol m^{-3}, $c_P^b = 8.47 \times 10^{-6}$ mol m^{-3}, $C = 1.000$ μF, and $U = 50.0$ kΩ.

potential window are natural choices for experiments in which it is hoped to measure both parameters. Chronopotentiometry and linear-scan voltammetry are two such methods, and each of these will be considered as candidate techniques. Conventional wisdom holds that chronopotentiometry is a robust voltammetric method when resistance is present whereas linear-scan voltammetry is badly corrupted by uncompensated resistance, because the linearity of the scan is destroyed. Potential-step voltammetry is not usually considered as a voltammetric method that sweeps the electrode potential but, when appreciable uncompensated resistance is present, a step to a judiciously chosen cell potential does indeed sweep the electrode through both the escarpment and plateau regions. In the latter circumstance, the name "ohmic-sweep voltammetry" has been attached to the "step" experiment.

Thus we will explore three candidate techniques: chronopotentiometry, linear-scan voltammetry, and potential-step voltammetry. That these are not as different as might be imagined is illustrated in Figure 1, which shows how the electrode potential is swept in each of the three methods. Note that each method has a characteristic parameter: the constant applied current I_{app} in chronoamperometry, the scan rate v in linear-scan voltammetry, and the step size E_{step} in potential-step voltammetry. For comparability, each of these parameters has been selected in Figure 1 so as to cause the electrode potential to sweep across the potential window in exactly 15 s.

MODELING THE VOLTAMMOGRAMS

The first step in our exercise is to simulate experimental voltammograms for each of the three techniques. By "voltammogram" in this context, we mean a graph of the cell potential E_{cell} versus time in the case of chronopotentiometry and a graph of the total cell current I_{cell} versus t for the other two techniques. We have devised a method, described in this section, that can accomplish this for any values of the double-layer capacitance C, the uncompensated resistance U, and the composite constant $nFAc_R^b(D_R)^{1/2}$ and for any one of the three candidate techniques.

The route that we follow in simulating the voltammograms is first to create a "universal voltammogram" from which, via convolutive modeling, the three technique-specific voltammograms can then be constructed.

Creating the Universal Voltammogram. The initial, null, potential E_n of the system can be described by Nernst's equation in terms of either the electrode reaction's conditional potential $E^{o\prime}$ or its half-wave potential $E_{1/2}$.

$$E_n = E^{o\prime} + \frac{RT}{nF}\ln\left\{\frac{c_P^b}{c_R^b}\right\} = E_{1/2} + \frac{RT}{nF}\ln\left\{\frac{c_P^b}{c_R^b}\sqrt{\frac{D_P}{D_R}}\right\} \quad (2)$$

Because we have postulated that the reaction be reversible, Nernst's law also holds when the electrode is working, with the relevant concentrations then being those of the product and reactant at the electrode surface, that we identify by a superscript s

$$E_n = E_{1/2} + \frac{RT}{nF}\ln\left\{\frac{c_P^s}{c_R^s}\sqrt{\frac{D_P}{D_R}}\right\} \quad (3)$$

It is well known[8,9] that, for electrode reaction 1 fed by planar semiinfinite diffusion, the equations

$$\frac{M_{far}}{nAF} = \sqrt{D_R}[c_R^b - c_R^s] = \sqrt{D_P}[c_p^s - c_p^b] \quad (4)$$

hold, where M_{far} is the semiintegral of the faradaic current I_{far},

$$M_{far} = \frac{d^{-1/2}}{dt^{-1/2}}I_{far} = \frac{1}{\sqrt{\pi}}\int_0^t I_{far}\frac{d\tau}{\sqrt{t-\tau}} \quad (5)$$

irrespective of other factors. These relationships presuppose that, prior to the start of the experiment at time $t = 0$, the concentrations of R and P are uniform and equal to their bulk values. Note that the electron number n is a signed quantity, being positive for an anodic reaction, when the current is also positive. The restriction to planar diffusion (sometimes ambiguously characterized as "linear diffusion" invalidates the application of our treatment to ultramicroelectrodes, to which transport is necessarily convergent.

Please appreciate that, when uncompensated resistance is present, a careful distinction needs to be drawn between the measured cell potential E_{cell} and the electrode potential E, which is not directly measurable and which appears in eq 3. It is useful to replace the variable E by a dimensionless equivalent

$$\epsilon = (nF/RT)(E - E_n) \quad (6)$$

In terms of this abbreviation, the relationship

(8) Oldham, K. B.; Spanier, J. *J. Electroanal. Chem.* **1970**, *26*, 331.
(9) Oldham, K. B.; Myland, J. C. *Fundamentals of electrochemical science*; Academic Press: San Diego, 1994.

$$\frac{nFAc_R^b\sqrt{D_R}}{M_{far}} = 1 + \frac{\exp\epsilon_{1/2} + 1}{\exp\epsilon - 1} \quad (7)$$

may be derived straightforwardly by combining eqs 2−4. Expression 7, in which $\epsilon_{1/2}$ abbreviates $nF(E_{1/2} - E_n)/RT$, applies to all three techniques and constitutes the universal voltammogram. Notice that the only variables in eq 7 are M_{far} and ϵ; the only other terms are $\epsilon_{1/2}$, which is readily calculable from $E_{1/2}$, and the composite constant $nFAc_R^b(D_R)^{1/2}$.

Relating the Technique-Specific Voltammograms to the Universal Voltammogram. In chronopotentiometry, a constant current I_{app} is applied through the cell and its passage through the uncompensated resistance U generates a constant difference UI_{app} between the cell potential and the electrode potential. Therefore

$$E_{cell} = UI_{app} + E = UI_{app} + E_n + RT\epsilon/nF \quad (8)$$

Not all the applied current flows through the faradaic pathway, however. A portion I_{cap}, equal to $C\mathrm{d}E/\mathrm{d}t$, where C is the capacitance, is diverted through the double-layer charging route. Accordingly

$$I_{far} = I_{app} - I_{cap} = I_{app} - C\frac{\mathrm{d}E}{\mathrm{d}t} = I_{app} - \frac{RTC}{nF}\frac{\mathrm{d}\epsilon}{\mathrm{d}t} \quad (9)$$

which gives

$$M_{far} = 2I_{app}\sqrt{\frac{t}{\pi}} - \frac{RTC}{nF}\frac{\mathrm{d}^{1/2}\epsilon}{\mathrm{d}t^{1/2}} \quad (10)$$

on semiintegration.

In linear-scan voltammetry, the cell current is driven through the uncompensated resistance by the difference between the applied cell potential $E_n + vt$ and the electrode potential E:

$$I_{cell} = \frac{E_n + vt - E}{U} = \frac{vt}{U} - \frac{RT\epsilon}{nFU} \quad (11)$$

An equation very similar to (9) applies in this case, except that the constant I_{app} is replaced by the time-dependent I_{cell}

$$I_{far} = I_{cell} - I_{cap} = \frac{vt}{U} - \frac{RT\epsilon}{nFU} - \frac{RTC}{nF}\frac{\mathrm{d}\epsilon}{\mathrm{d}t} \quad (12)$$

Semiintegration yields

$$M_{far} = \frac{4v}{3U}\sqrt{\frac{t^3}{\pi}} - \frac{RT}{nFU}\frac{\mathrm{d}^{-1/2}\epsilon}{\mathrm{d}t^{-1/2}} - \frac{RTC}{nF}\frac{\mathrm{d}^{1/2}\epsilon}{\mathrm{d}t^{1/2}} \quad (13)$$

an equation in which three time-dependent terms occupy the right-hand side.

The derivation for potential-step voltammetry parallels that for linear-scan voltammetry except that a constant E_{step} replaces vt. The final equations are

$$I_{cell} = \frac{E_{step}}{U} - \frac{RT\epsilon}{nFU} \quad (14)$$

and

$$M_{far} = \frac{2E_{step}}{U}\sqrt{\frac{t}{\pi}} - \frac{RT}{nFU}\frac{\mathrm{d}^{-1/2}\epsilon}{\mathrm{d}t^{-1/2}} - \frac{RTC}{nF}\frac{\mathrm{d}^{1/2}\epsilon}{\mathrm{d}t^{1/2}} \quad (15)$$

Notice that in deriving eqs 10, 13, and 15 we used the rule that $(\mathrm{d}^{-1/2}/\mathrm{d}t^{-1/2})(\mathrm{d}/\mathrm{d}t)\,f(t) = (\mathrm{d}^{1/2}/\mathrm{d}t^{1/2})\,f(t)$. This rule does *not* apply generally, but it is valid when, as with ϵ here, the function $f(t)$ is zero at $t = 0$.

At this stage we have a means, namely, eq 7, of constructing the M_{far} versus ϵ relationship from known data. We also have equations, namely, eq 10, 13, or 15, for relating M_{far} to ϵ and t, as well as equations, namely, eq 8, 12, or 14, by which ϵ and t are related to the experimental observable, either E_{cell} or I_{cell}. In principle, therefore, the technique-specific voltammograms, i.e., plots of E_{cell} or I_{cell} versus t, are accessible to simulation. The sought relationships were derived numerically, using the method described below for linear-sweep voltammetry.

Generating Technique-Specific Voltammograms via Convolutive Modeling. Let Δ be a small time interval equal to t/J and let $\epsilon_1, \epsilon_2, ..., \epsilon_j, ..., \epsilon$ denote the values of ϵ at times $\Delta, 2\Delta, ..., j\Delta, ..., J\Delta$, Note that $\epsilon_0 = 0$ because $E = E_n$ initially and that $\epsilon_J = \epsilon$, the value at time t. In this circumstance, the RL algorithm[10] provides the following expressions for the semiderivative and semiintegral of ϵ at time t

$$\frac{\mathrm{d}^{\pm1/2}\epsilon}{\mathrm{d}t^{\pm1/2}} = \frac{8\Delta^{\mp1/2}}{(5 \mp 1)\sqrt{\pi}}\left[\epsilon + \sum_{j=1}^{J-1}\epsilon_{J-j}\{(j+1)^{1\mp1/2} - 2j^{1\mp1/2} + (j-1)^{1\mp1/2}\}\right] \quad (16)$$

For linear-scan voltammetry, this may be combined with eqs 7 and 13 to generate the elaborate, but uncomplicated, result

$$\frac{n^2F^2Ac_R^b}{4RTC}\sqrt{\frac{\pi D_R}{\Delta}}\frac{\exp\epsilon - 1}{\exp\epsilon_{1/2} + \exp\epsilon} + \frac{\epsilon}{3UC} + \frac{\epsilon}{2\Delta} = \frac{J^{3/2}nFv\Delta}{3RTUC} - \sum_{j=1}^{J-1}\epsilon_{J-j}\left\{\frac{(j+1)^{3/2} - 2j^{3/2} + (j-1)^{3/2}}{3UC} + \frac{(j+1)^{1/2} - 2j^{1/2} + (j-1)^{1/2}}{2\Delta}\right\} \quad (17)$$

In this form, the present (i.e., $t = J\Delta$) value of ϵ is found exclusively on the left-hand side of the equation, whereas all previous ($j = 1, 2, ..., J - 1$) values are found solely on the right-hand side. Hence, for known parameter values, the right-hand side is calculable numerically, and ϵ can then be found by a simple iterative numerical "hunt", using the bisection method.[11] In this way, values of ϵ at a sequence of closely spaced times, spanning the entire

(10) Oldham, K. B.; Spanier, J. *The fractional calculus*; Academic Press: New York and London, 1974; p 146.

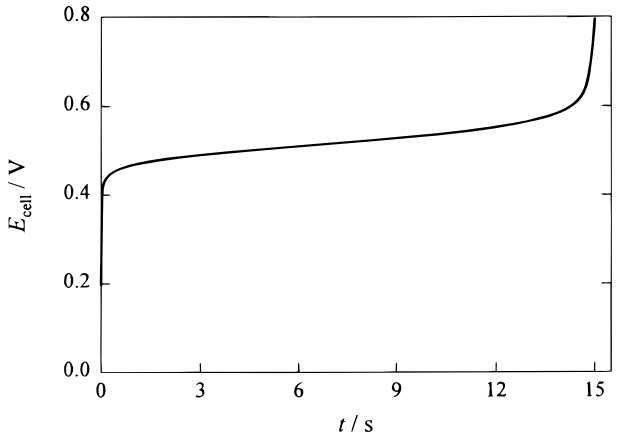

Figure 2. A chronopotentiogram for an uncompensated resistance of 15.0 kΩ, c_R^b = 5.00 mol m^{-3}, and I_{app} = 13.03 μA. Other parameters as in Figure 1. The ordinate is the measured cell potential, *not* the electrode potential.

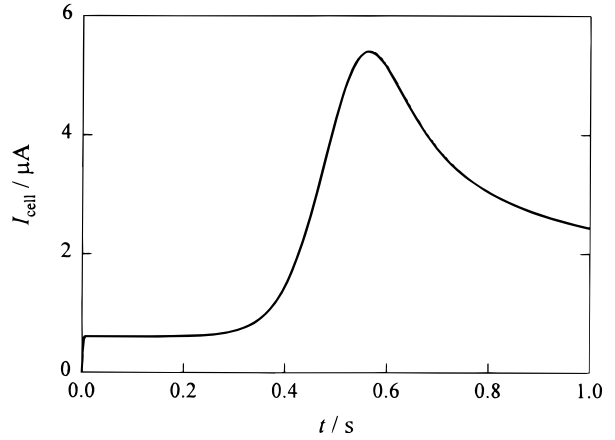

Figure 3. A linear-scan voltammogram for an uncompensated resistance of 1.50 kΩ, c_R^b = 0.200 mol m^{-3}, and v = 0.604 V s^{-1}. Other parameters as in Figure 1.

experiment, may be calculated. This is the procedure that we used to generate ϵ versus t data at 750 equally spaced instants in time.

With ϵ known as a function of time, it is now straightforward to calculate, via eq 11, I_{cell} as a function of time. That is, the entire linear-scan voltammogram, incorporating the effects of double-layer capacitance and uncompensated resistance, may be constructed. The procedure for the chronopotentiometric and potential-step techniques is similar, but somewhat simpler.

Because we wished to intercompare voltammograms that traversed the standard (600/n) millivolt window in one of three standard time intervals of 1.000, 5.000, or 15.00 s, we adjusted the technique-specific parameter (I_{app}, v, or E_{step}) to accomplish this standardization. Examples of voltammograms constructed in this way are shown as Figures 2−4. We invariably adopted the values n = 1, $A = 3.698 \times 10^{-6}$ m^2, T = 298.15 K, $D_R = 1.000 \times 10^{-9}$ m^2 s^{-1}, E_n = 0.000 V, and $nE_{1/2}$ = 0.300 V, the last two implying $c_P^b = (8.47 \times 10^{-6})c_R^b$. Generally we used C = 1.000 μF, corresponding to a specific capacitance of ~27 μF cm^{-2}, a typical value for a mercury/aqueous solution interface and many other

(11) Press, W. H.; Flannery, B. P.; Teukolsky, S. A.; Vetterling, W. T. *Numerical recipes. The art of scientific computing*; Cambridge University Press: Cambridge, U.K., 1986; p 579.

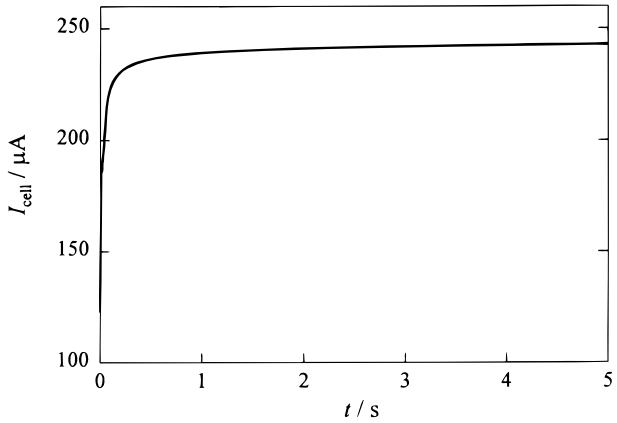

Figure 4. A potential-step voltammogram for an uncompensated resistance of 5.00 kΩ, c_R^b = 1.000 mol m^{-3}, and E_{step} = 0.614 V. Other parameters as in Figure 1.

interfaces. We used various values of U and c_R^b, as reported below.

ANALYSIS OF THE TECHNIQUE-SPECIFIC VOLTAMMOGRAMS

The voltammograms constructed as explained above mimic ideal experimental voltammograms. Our goal is to determine whether, despite the substantial presence of capacitive and resistive interference in the faradaic process, we can nevertheless recover useful values of $E_{1/2}$ and c_R^b. We therefore need to analyze the technique-specific voltammograms to recover values of the sought quantities. Before we proceed to that step, however, we need to answer two pertinent questions: How will the voltammograms be analyzed to extract $E_{1/2}$ and c_R^b, and do we assume that U and C have known values?

Very diverse methods are used to analyze chronopotentiograms, linear-scan voltammograms, and potential-step voltammograms, and none of these is guaranteed to work when uncompensated resistance and/or double-layer capacitance are/is present. Therefore, we devised a new analytical method that applies even-handedly to all of our three candidate methods. In effect, this method converts the technique-specific voltammograms to the universal voltammogram and analyzes that.

Method of Analyzing the Technique-Specific Voltammograms. Equation 7 contains only two variables—the faradaic semiintegral M_{far} and the parameter ϵ, reflecting the electrode potential. The equation shows that a linear relationship exists between $1/M_{far}$ and $1/(\exp\epsilon - 1)$. Thus, a plot of the former versus the latter would produce a straight line with the characteristics shown in Figure 5. A similar analysis has found utility previously,[12,13] in the context of "global analysis". The data points in such a plot, or in a corresponding regression are, of course, equally spaced *in time*, not in either one of the axial variables. One method of estimating the composite constant $nFAc_R{}^b(D_R)^{1/2}$ and $\epsilon_{1/2}$ would be via the standard "least-squares" formulas based

(12) Bond, A. M.; Mahon, P. J.; Oldham, K. B.; Zoski, C. G. *J. Electroanal. Chem.* **1994**, *366*, 15.

(13) Bond, A. M.; Mahon, P. J.; Maxwell, E. A.; Oldham, K. B.; Zoski, C. G. *J. Electroanal. Chem.* **1994**, *370*, 1.

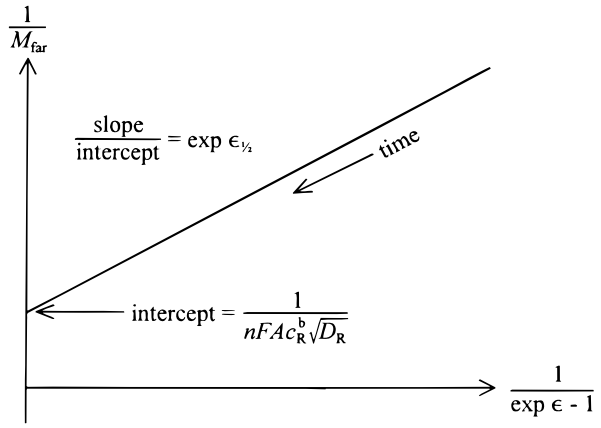

Figure 5. An illustration of the linear relationship between the reciprocals of the faradaic semiintegral M_{far} and ($\exp\epsilon - 1$) where $\epsilon = nF(E - E_n)/RT$.

on N data points, namely

$$nFAc_R^b\sqrt{D_R} = \frac{1}{\text{intercept}} = \frac{N\sum x^2 - (\sum x)^2}{\sum x^2 \sum y - \sum x \sum xy} \quad (18)$$

and

$$\exp\left\{\frac{nF}{RT}(E_{1/2} - E_n)\right\} = \frac{\text{slope}}{\text{intercept}} = \frac{N\sum xy - \sum x \sum y}{\sum x^2 \sum y - \sum x \sum xy} \quad (19)$$

where $x = 1/(\exp\epsilon - 1)$ and $y = 1/M_{far}$. However, these formulas would place too much emphasis on the short time points, which lie in the "northeast" region of the Figure 5 graph and which are most likely to be in error. In this circumstance, a weighted least-squares approach is called for. If (without justification) we assume that the same fractional uncertainty is associated with each "measurement" of $1/M_{far}$, then an appropriate weight to attach to each datum would be $(M_{far})^2$ or $1/y^2$. With this adjustment, the formulas for calculating $nFAc_R^b(D_R)^{1/2}$ and $E_{1/2}$ become

$$nFAc_R^b\sqrt{D_R} = \frac{\sum(1/y)^2 \sum(x/y)^2 - [\sum(x/y^2)]^2}{\sum(x/y)^2 \sum(1/y) - \sum(x/y^2)\sum(x/y)} \quad (20)$$

and

$$\exp\left\{\frac{nF}{RT}(E_{1/2} - E_n)\right\} = \frac{\sum(1/y)^2 \sum(x/y) - \sum(x/y^2)\sum(1/y)}{\sum(x/y)^2 \sum(1/y) - \sum(x/y^2)\sum(x/y)} \quad (21)$$

The similarly weighted correlation coefficient, a measure of how linear the relationship is in practice, may be calculated as

$$r = \frac{\sum(1/y)^2 \sum(x/y) - \sum(x/y^2)\sum(1/y)}{\sqrt{\{\sum(1/y)^2 \sum(x/y)^2 - [\sum(x/y^2)]^2\}\{N\sum(1/y)^2 - [\sum(1/y)]^2\}}} \quad (22)$$

With these replacement formulas, greater weight is placed on data close to the escarpment region. To check these procedures, we used them to recover known values of $E_{1/2}$ and of the composite constant from typical voltammograms. The success of this operation is evident from Table 1. Of course, we used the exactly known values of the uncompensated resistance U and the double-layer capacitance C in this exercise.

We routinely used eqs 20 and 21 to recover, or to attempt to recover, values of $nFAc_R^b(D_R)^{1/2}$ and $E_{1/2}$ from technique-specific voltammograms when correct values of U and C were used and when they were not. Of course it was first necessary to calculate M_{far} versus ϵ data from the simulated voltammograms. This was accomplished as follows: *for chronopotentiometry*, by use of the equation

$$\epsilon = (nF/RT)(E_{cell} - UI_{app} - E_n) \quad (23)$$

and then eq 10; *for linear-scan voltammetry*, by use of the equation

$$\epsilon = (nF/RT)(vt - UI_{cell}) \quad (24)$$

followed by eq 13; *and for potential-step* voltammetry, by use of the equation

$$\epsilon = (nF/RT)(E_{step} - UI_{cell}) \quad (25)$$

and then eq 15. Equations 23−25 follow straightforwardly from eqs 8, 11, and 14, respectively. In performing the regression, we used the data from the entire $(600/n)$ mV window in the cases of chronopotentiometry and potential-step voltammetry, but only the final three-fourths of the data were used in the case of linear-scan voltammetry. The reason for the different treatments can be appreciated from Figure 1. For chronopotentiometry and potential-step voltammetry, there is an almost immediate entry, following the $t = 0$ initiation of the experiment, to the escarpment region. This is not the case in linear-scan voltammetry, during approximately the first quarter of which experiments no faradaic current flows and therefore no purpose is served by including such data in the analysis.

Degree of Certitude in the Capacitance and Resistance. Early in this section two questions were posed. The first is now answered. The second asked whether it should be supposed that the experimenter was ignorant of the values of U and C, or if s/he could be assumed to know these values. In principle, it is possible to use the information present in the voltammogram to elucidate the four parameters c_R^b, $E_{1/2}$, U, and C. In practice, though, it would be folly to expect that four parameters could be extracted from data of the quality typical of electrochemical measurements. On the other hand, it would be very unusual for a voltammetrist to have precise knowledge of the double-layer capacitance and the uncompensated resistance when setting out to perform an

Table 1. A Demonstration of the Efficiency with Which the Analysis Routine Can Recover Values of the Reactant Concentration and the Half-Wave Potential[a]

technique	technique-specific parameter	t_{max}/s	U/kΩ	recovered c_R^b/mol m^{-3}	recovered $E_{1/2}$/mV	correlation coefficient r
chronopotentiometry	$I_{app} = 4.68960\ \mu$A	5	50	1.000 013 3	300.0018	0.999 999 799
linear-scan voltammetry	$v = 0.0866630$ V s^{-1}	15	200	0.999 999 4	300.0002	1
potential-step voltammetry	$E_{step} = 0.699663$ V	1	15	1.000 001 2	300.001	0.999 999 948

[a] The correct values of these parameters are $c_R^b = 1.000\ 000\ 0$ mol m^{-3} and $E_{1/2} = 300.0000$ mV.

experiment aimed at determining either $E_{1/2}$ or c_R^b. Accordingly, we made an intermediate assumption: that *approximate* values of U and C are known a priori.

We do not attach any specific uncertainties to the knowledge of the electrical elements. Instead we decided to ask, "How much error will be introduced into $E_{1/2}$ or c_R^b by a very small error in U (or C)?". Specifically, we sought to determine numerical values (including the sign) of the four partial derivatives, the so-called "sensitivity indices".

$$\frac{nFU}{RT}\frac{\partial E_{1/2}}{\partial U} \quad \text{or} \quad \frac{\partial \epsilon_{1/2}}{\partial \ln U} \tag{26}$$

$$\frac{U}{c_R^b}\frac{\partial c_R^b}{\partial U} \quad \text{or} \quad \frac{\partial \ln c_R^b}{\partial \ln U} \tag{27}$$

$$\frac{nFC}{RT}\frac{\partial E_{1/2}}{\partial C} \quad \text{or} \quad \frac{\partial \epsilon_{1/2}}{\partial \ln C} \tag{28}$$

$$\frac{C}{c_R^b}\frac{\partial c_R^b}{\partial C} \quad \text{or} \quad \frac{\partial \ln c_R^b}{\partial \ln C} \tag{29}$$

Such a search is known as a "sensitivity analysis" of the data.

Scope of the Sensitivity Analysis. Because the object of our study is to compare three voltammetric techniques, we analyzed the voltammograms produced by each technique in exactly the same fashion. We determined the small error introduced into $\epsilon_{1/2}$ or c_R^b by a small error in U or C, expressing the results as in eqs 26−29. We carried out 45 trials. Each trial consists of selecting every possible combination of values from the following possibilities:

$$t_{max} = \text{duration of the experiment} = 1.000, 5.000, \text{or } 15.00 \text{ s} \tag{30}$$

$$\text{composite constant} = nFAc_R^b\sqrt{D_R} = 5.64 \times 10^{-5}, 1.13 \times 10^{-5}, \text{ or } 2.26 \times 10^{-6} \text{ A s}^{1/2} \tag{31}$$

corresponding to $c_R^b = 5.00$, 1.00, or 0.200 mol m^{-3}

$$U = \text{uncompensated resistance} = 1.500, 5.000, 15.00, 50.00, \text{or } 200.0 \text{ kΩ} \tag{32}$$

Because of the increased likelihood of interference by natural convection at long times, no studies were conducted for $t_{max} > 15$ s. Values of t_{max} represent typical experimental durations. The value of the double-layer capacitance C was not varied, being always 1.000 μF. Each of the four sensitivity indices was measured for each of the three voltammetric techniques, a total of 540 measurements. Before each trial it was necessary to adjust I_{app}, v, and E_{step} to the values necessary to ensure that the duration of each experiment, i.e., the time to sweep across the $(600/n)$ mV window, conformed to the chosen value from the set in eq 30.

Taking sensitivity index 27 as an example, it was measured in the following way. First, an exact, technique-specific voltammogram was generated as described in Modeling the Voltammograms. . Then, this voltammogram was analyzed as described in Analysis of the Technique-Specific Voltammograms, using a slightly erroneous value, $U + \delta U$, of the uncompensated resistance. δU was typically $\pm U/10000$. This error leads to a consequential error, δc_R^b. The term $(U/c_R^b)/(\delta c_R^b/\delta U)$ was accepted as the true value of the sensitivity index, $(U/c_R^b)/(\partial c_R^b/\partial U)$, provided that a smaller value of δU had no significant effect and that the correlation coefficient, r, exceeded 0.99. In ∼30% of the potential step and chronopotentiometry cases, this procedure failed to give an acceptable result: these cases were excluded from further consideration. There were no failures in the analysis of linear-scan voltammograms.

RESULTS AND CONCLUSIONS

We expected the sensitivity indices to reflect the choice of parameters from eqs 30−32 in the ways described below. Sensitivity analysis uses the terms "fragile" and "robust" to imply high- and low-sensitivity indices, respectively.

General Trends. When the uncompensated resistance is small we expect robustness, i.e., a small sensitivity index, signifying that a large fractional error in U would lead to only small errors in the recovered values of $\epsilon_{1/2}$ and c_R^b. Conversely, we predicted that the analysis would be fragile; i.e., the sensitivity indices $\partial\epsilon_{1/2}/\partial \ln U$ and $\partial \ln c_R^b/\partial \ln U$ would be large, for a large uncompensated resistance. We found these expectations to be fulfilled universally. For example, Table 2 shows a steady increase in fragility for $\partial\epsilon_{1/2}/\partial \ln U$ with increasing uncompensated resistance, for all three methods. Note, however, that chronopotentiometry and potential-step voltammetry are superior to linear-scan voltammetry by ∼1 order of magnitude, for the particular set of conditions presented.

A second expectation was that robustness would improve with increasing concentration. One reason for this belief is that the faradaic current scales with concentration and therefore increasingly dominates the concentration-independent capacitive current. Our finding is that this is always true for chronopotentiometry

Table 2. Sensitivity Indices for the Three Techniques When $t_{max} = 5.00$ s and $c_R^b = 5.000$ mol m^{-3}

	$\partial \ln c_R^b / \partial \ln U$		
U/kΩ	chrono-potentiometry	linear-scan voltammetry	potential-step voltammetry
1.5	−0.016	0.18	−0.013
5	−0.53	0.79	−0.025
15	−0.16	3	−0.13
50	−0.53	9.3	−0.58
200	−2.1	33	−2.2

Table 3. Comparison of the Sensitivity Indices for the Three Techniques When $U = 15$ kΩ, $t_{max} = 5.00$ s, and $c_R^b = 1.000$ mol m^{-3}

	$\partial\epsilon_{1/2}/\partial \ln U$	$\partial \ln c_R^b/\partial \ln U$	$\partial\epsilon_{1/2}/\partial \ln C$	$\partial \ln c_R^b/\partial \ln C$
chronopotentiometry	−71	−15	41	9.1
linear-scan voltammetry	−0.88	0.41	0.63	0.07
potential-step voltammetry	−17	−0.045	2.1	0.008

and always true for sensitivity indices $\partial\epsilon_{1/2}/\partial \ln C$ and $\partial \ln c_R^b/\partial \ln C$ but not necessarily true for indices $\partial\epsilon_{1/2}/\partial \ln U$ and $\partial \ln c_R^b/\partial \ln U$, for linear-scan and potential-step voltammetries.

A third prediction was that increasing experimental duration would improve robustness. The reason for this is that the *UC* time constant is then a smaller fraction of the experimental time scale. This turns out to be generally true, except for index $\partial \ln c_R^b/\partial \ln C$ in the cases of linear-scan and potential-step voltammetries, where a variety of behaviors is observed.

Representative Results. It is not practical to present all 540 measurements of the sensitivity indices here. However, they are available for inspection on the Internet.[14] Moreover, Table 3 lists our results for a single, typical trial. The parameters chosen for the tabulated trial are the medians of the t_{max}, c_R^b, and U values investigated in this study, as listed in eqs 30−32. Contrary to our expectation, chronopotentiometry is invariably the most fragile of the techniques in this comparison.

In fact, in terms of the sensitivity indices, chronopotentiometry turns out to be the "worst" of the three methods except in the long-time, high-concentration region where it is superior in terms of index $\partial \ln c_R^b/\partial \ln U$. An example of the simulated experimental chronopotentiogram, under these conditions, is shown in Figure 2. The four sensitivity indices derived from this curve are $\partial\epsilon_{1/2}/\partial \ln U = -7.7$, $\partial \ln c_R^b/\partial \ln U = -0.014$, $\partial\epsilon_{1/2}/\partial \ln C = 0.069$, and $\partial \ln c_R^b/\partial \ln C = 0.014$.

Optimal Technique for Determining $E_{1/2}$. We found that linear-scan voltammetry was the most robust method for measuring the half-wave potential; i.e., values of indices $\partial\epsilon_{1/2}/\partial \ln U$ and $\partial\epsilon_{1/2}/\partial \ln C$, for this technique, were invariably smaller than those for chronopotentiometry or potential-step voltammetry. Figure 3 shows an example of a linear-scan voltammogram for the conditions given in the caption. The conditions of short time and low concentration used for the voltammogram in Figure 3 are particularly difficult; nevertheless, the sensitivity index $\partial\epsilon_{1/2}/\partial \ln U$ has the robust value of −0.14. On the other hand, the sensitivity index $\partial\epsilon_{1/2}/\partial \ln C$ has the fragile value of 12.1; even so, it is superior to the corresponding values of the rival techniques. The other two sensitivity indices for this voltammogram are $\partial \ln c_R^b/\partial \ln U = -0.012$ and $\partial \ln c_R^b/\partial \ln C = 0.73$.

Optimal Techniques for Determining c_R^b. The decision as to which is the best technique for measuring the reactant concentration is less clear-cut than for $E_{1/2}$. All that can be categorically stated is that chronopotentiometry is a poor choice, other than in the special case of long time and high concentration. For concentrations not less than 1 mol m^{-3}, potential-step voltammetry is generally the best method of the three. Figure 4 shows the voltammogram for a case in point. Robustness is indicated in the values $\partial \ln c_R^b/\partial \ln U = -0.019$ and $\partial \ln c_R^b/\partial \ln C = -0.025$. On the other hand, this would be a poor voltammogram from which to calculate $E_{1/2}$ since $\partial\epsilon_{1/2}/\partial \ln U = -12$ and $\partial\epsilon_{1/2}/\partial \ln C = 1.3$.

SUMMARY AND DISCUSSION

On the basis of our sensitivity indices, the answers we can give to the question that forms the title of this article are as follows: (1) Overall, linear-scan voltammetry is the best method and, surprisingly, chronopotentiometry the worst. (2) Only at rather high reactant concentrations and long experiment times is chronopotentiometry satisfactory and only then for determining the composite constant, not $E_{1/2}$. (3) For determining the half-wave potential, linear-scan voltammetry is invariably the method of choice. (4) For measuring the composite constant $nFAc_R^b(D_R)^{1/2}$, linear-scan voltammetry is the best technique for tolerating high resistance, often performing robustly even for rapid experiments at low reactant concentrations. (5) At moderate levels of uncompensated resistance, potential-step (or ohmic-sweep) voltammetry frequently outperforms linear-scan voltammetry in the measurement of the composite constant. To our knowledge, potential-step voltammetry has never been used in this way.

This has been purely a modeling study, and we are unable to predict whether our conclusions will satisfactorily carry over into the experimental domain. Among the shortcomings that we acknowledge are the following: (1) Double-layer capacitance has been assumed independent of the electrode potential, possibly an oversimplification. (2) We have not investigated the effect of changing the width of the $(600/n)$ millivolt "window" or of making it asymmetric with respect to the half-wave potential. (3) Our technique-specific voltammograms have been *ideal*. Experimental scatter has not been introduced and its effects remain unknown. (4) We have analyzed all three technique-specific voltammograms in the same way. By focusing only on certain regions of the voltammogram, other methods of analysis could possibly lead to other conclusions.

It is tempting to associate finite quantitivity with a sensitivity index. Thus, $\partial \ln c_R^b/\partial \ln U = -0.10$ could be taken to imply that a 20% overestimate of the uncompensated resistance would lead to a concentration measurement that is 2% low. Such an inference assumes that $\Delta \ln c_R^b/\Delta \ln U = \partial \ln c_R^b/\partial \ln U$, which is not necessarily valid. Likewise it would be incautious to suppose that $\partial\epsilon_{1/2}/\partial \ln C = \pm 0.10$ always means that a 10% error in estimating the double-layer capacitance will lead to a 2.6 mV discrepancy between the true and the measured half-wave potentials.

(14) www.trentu.ca/chemistry/oldham/Paper189.

Notwithstanding these caveats, we believe that this study has been successful in the following: (1) developing a highly accurate way of simulating various types of reversible voltammetry, with incorporation of the effects of uncompensated resistance and double-layer capacitance of any magnitudes; (2) introducing a new method of analyzing reversible voltammograms and chronopotentiograms (The method utilizes all the information content of the voltammogram and employs statistical weighting.); (3) applying sensitivity analysis to identify cause-and-effect relationships between voltammetric parameters; (4) suggesting that linear-scan voltammetry, rather than chronopotentiometry, may be the voltammetric method of choice when uncompensated resistance is present; (5) demonstrating a new and valuable role for potential-step voltammetry.

ACKNOWLEDGMENT

Financial support from the Natural Sciences and Engineering Research Council of Canada is gratefully acknowledged.

Received for review December 7, 1999. Accepted April 20, 2000.

AC991400B